AGU PUBLICATIONS

JGR

Journal of Geophysical Research: Oceans

RESEARCH ARTICLE

10.1002/2017JC013412

The Role of the New Zealand Plateau in the Tasman Sea Circulation and Separation of the East Australian Current

Christopher Y. S. Bull[1,2], Andrew E. Kiss[2,3,4], Erik van Sebille[2,5,6], Nicolas C. Jourdain[2,7], and Matthew H. England[1,2]

[1]Climate Change Research Centre, University of New South Wales, Sydney, NSW, Australia, [2]ARC Centre of Excellence for Climate System Science, University of New South Wales, Sydney, NSW, Australia, [3]School of Physical, Environmental and Mathematical Sciences, University of New South Wales Canberra at the Australian Defence Force Academy, Canberra, ACT, Australia, [4]Research School of Earth Sciences, Australian National University, Canberra, ACT, Australia, [5]Grantham Institute and Department of Physics, Imperial College London, London, United Kingdom, [6]Institute for Marine and Atmospheric Research Utrecht, Utrecht University, Utrecht, The Netherlands, [7]Univ. Grenoble Alpes, CNRS, IRD, IGE, Grenoble, France

Key Points:
- EAC separation latitude shifts south 1.1 degrees when the New Zealand submarine platform is completely removed and Tasman Sea is leveled
- The presence of the New Zealand submarine platform weakens the EAC extension and strengthens the Tasman Front
- Meridional gradients in the basin-wide wind stress curl are not the sole factor determining the mean latitude of EAC partial separation

Correspondence to:
C. Y. S. Bull,
christopher.ys.bull@gmail.com

Citation:
Bull, C. Y. S., Kiss, A. E., van Sebille, E., Jourdain, N. C., & England, M. H. (2018). The role of the New Zealand plateau in the Tasman Sea circulation and separation of the East Australian Current. *Journal of Geophysical Research: Oceans*, *123*, 1457–1470. https://doi.org/10.1002/2017JC013412

Received 27 SEP 2017
Accepted 5 JAN 2018
Accepted article online 11 FEB 2018
Published online 27 FEB 2018

Abstract The East Australian Current (EAC) plays a major role in regional climate, circulation, and ecosystems, but predicting future changes is hampered by limited understanding of the factors controlling EAC separation. While there has been speculation that the presence of New Zealand may be important for the EAC separation, the prevailing view is that the time-mean partial separation is set by the ocean's response to gradients in the wind stress curl. This study focuses on the role of New Zealand, and the associated adjacent bathymetry, in the partial separation of the EAC and ocean circulation in the Tasman Sea. Here utilizing an eddy-permitting ocean model (NEMO), we find that the complete removal of the New Zealand plateau leads to a smaller fraction of EAC transport heading east and more heading south, with the mean separation latitude shifting >100 km southward. To examine the underlying dynamics, we remove New Zealand with two linear models: the Sverdrup/Godfrey Island Rule and NEMO in linear mode. We find that linear processes and deep bathymetry play a major role in the mean Tasman Front position, whereas nonlinear processes are crucial for the extent of the EAC retroflection. Contrary to past work, we find that meridional gradients in the basin-wide wind stress curl are not the sole factor determining the latitude of EAC separation. We suggest that the Tasman Front location is set by either the maximum meridional gradient in the wind stress curl or the northern tip of New Zealand, whichever is furthest north.

1. Introduction

Subtropical western boundary current (WBC) regions are warming 2–3 times faster than the globally averaged surface ocean warming rate (Wu et al., 2012; Yang et al., 2016).The intensification and poleward shift in separation of WBCs is thus an important problem to study, but our current understanding is hampered by limited historical measurements as well as a lack of regionally relevant modeling studies addressing a range of factors thought to influence separation (e.g., bathymetry, model resolution, sidewall boundary condition, and wind stress). In the Australian context, the poleward shift in the westerlies (Swart & Fyfe, 2012)—driven by both ozone depletion and greenhouse gas increases—is thought to be driving a change in the South Pacific wind stress curl field leading to an enhancement or "spin-up" of the EAC extension (Cai et al., 2005; Feng et al., 2016; Oliver & Holbrook, 2014; Ridgway, 2007; Ridgway et al., 2008; Roemmich et al., 2016; Sloyan & O'Kane, 2015). It is an open question as to whether the entire EAC spins up, or the EAC extension alone (Cetina-Heredia et al., 2014; Feng et al., 2016; Ridgway, 2007; Sloyan & O'Kane, 2015).

A widely held explanation for the latitude of separation (based on the Sverdrup (1947) balance) is that the *partial* separation of the East Australian Current (EAC) is determined by the steepest meridional gradient in the Pacific basin zonal-averaged wind stress curl (Bostock et al., 2006; Oliver & Holbrook, 2014; Tilburg et al., 2001). Similar linear assumptions are used in global studies; for example Wu et al. (2012) use the midlatitude zero wind stress curl line to explain shifts in the boundary between the subtropical and subpolar gyres. Despite well-known issues in using linear theory in western boundary current regions (e.g., vorticity advection, see Gray & Riser, 2014; Pedlosky, 1996; Thomas et al., 2014), climate change attribution studies often

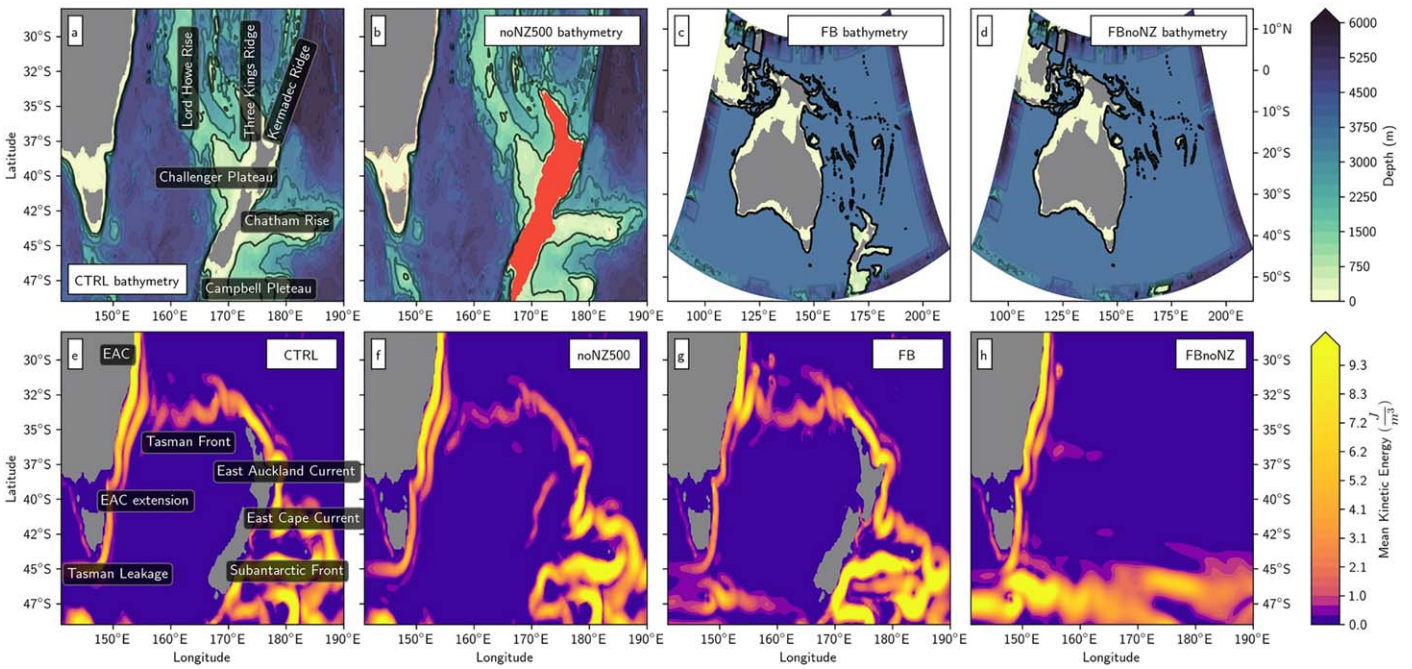

Figure 1. (a–d) Bathymetry of the experiments, solid contours are at 1, 2, 3, and 4 km. Figure 1b has an additional red filled contour to indicate 500 m isobath around New Zealand which was excavated. Regional NEMO modeling domain pictured in Figures 1c and 1d. (e–h) Volume-averaged mean kinetic energy down to 1,945 m.

resort to linear dynamics (e.g., Cai, 2006; Hill et al., 2011; Oliver & Holbrook, 2014; Sen Gupta et al., 2016) when relating the spin-up of the EAC to anthropogenic changes in the South Pacific wind stress curl.

The EAC system is the most energetic circulation feature in the south western Pacific Ocean and is a primary conduit for poleward heat transport from the tropics to midlatitudes (Hu et al., 2015; Ridgway & Dunn, 2003; Sloyan et al., 2016). The EAC system (summarized in Figure 1e) consists of a relatively steady upstream current (22.1 $\pm$ 7.5 Sv at 27°S; Sloyan et al., 2016), which partially bifurcates at 30°S–34°S (Cetina-Heredia et al., 2014). The branch that flows east forms the Tasman Front (Sutton & Bowen, 2014) and contributes to New Zealand's boundary currents, including the East Auckland Current and East Cape Current (Chiswell et al., 2015). In the process of separation, the EAC sheds an anticyclonic eddy (average radius 95 km; Everett et al., 2012) every ~100 days (Mata et al., 2006). Once the eddy detaches from the main current, the EAC then retracts northward (Mata et al., 2006) and it is this nonlinear eddy-dominated asymmetric oscillation that defines the time-mean partial separation latitude. The shed eddies then move south-westward in a procession that characterizes the EAC extension (Andrews & Scully-Power, 1976; Everett et al., 2012; Nilsson & Cresswell, 1980). A small portion of these eddies then continue around Tasmania (Pilo et al., 2015), at times making it as far westward as the Indian Ocean; the latter pathway is known as the Tasman Leakage (van Sebille et al., 2012). Via Tasman Leakage, the EAC participates in the Southern Hemisphere supergyre circulation (Ridgway & Dunn, 2007; Speich et al., 2007). Hill et al. (2011) found that the EAC extension and Tasman Front transport are anticorrelated in response to basin-scale winds with a time lag of ~3 years. Using observations and models, several other studies (Chiswell & Sutton, 2015; Hu et al., 2015; Oliver & Holbrook, 2014; Sloyan & O'Kane, 2015) have made similar findings; however, the underlying roles of nonlinear dynamics and bathymetry warrant further investigation.

Previous studies have suggested that New Zealand may be important for the EAC's separation latitude and Tasman Sea circulation (Heath, 1985; Warren, 1970). Prior to direct satellite observations, Warren (1970) suggested that mass balance requires the existence of a Tasman Front to satisfy Sverdrup (1947) transport constraints. Although Warren (1970) did not state it in these terms, subsequent authors (e.g., Godfrey et al., 1980; Tilburg et al., 2001) portrayed Warren (1970) as arguing that New Zealand has this putative effect by blocking westward-propagating Rossby waves. Godfrey et al. (1980) left open the possibility that New Zealand's blocking of Rossby waves determines the general region in which EAC separation can occur but

argued that the specific location of separation is controlled locally by coastline shape (particularly Sugarloaf Point). Tilburg et al. (2001) investigated the Tasman Sea circulation in a hierarchy of models of increasing realism but studied the removal of New Zealand only in the simplest of these: a linear, 1.5 layer, Sverdrup-Munk (Munk, 1950; Sverdrup, 1947) model. In this idealized model, the removal of New Zealand did not affect the separation latitude, and the authors invoked Sverdrup theory to suggest that the partial separation of the EAC can be explained by a steep meridional gradient at that latitude in the zonally integrated Hellerman and Rosenstein (1983) wind stress curl data set they used. However, linear models have been shown to lack skill in predicting changes in the EAC separation latitude (Oliver & Holbrook, 2014) and circulation changes in the Tasman Sea (Couvelard et al., 2008; Ridgway & Godfrey, 1994; Sen Gupta et al., 2016).

Our primary focus here is to investigate the role of New Zealand, and the associated adjacent bathymetry, in the partial separation of the EAC and circulation of the Tasman Sea. We aim to improve our understanding of the underlying dynamics of the EAC and other aspects of Tasman Sea circulation. We improve on Tilburg et al. (2001) by utilizing a full primitive equation eddy-permitting model that includes nonlinear dynamics and bottom topography. By removing New Zealand while retaining virtually the same atmospheric forcing, we are able to diagnose the impact of the bathymetry around New Zealand, without confounding changes in the wind stress curl. Using NEMO, we present a suite of experiments with modified bathymetry in the Tasman Sea (section 2.2) to investigate the relationship between the EAC separation latitude and New Zealand (section 4). Contrary to Tilburg et al. (2001), we find that bottom topography and nonlinear effects are important for the EAC separation location.

2. Ocean Model and Experimental Design

2.1. The Ocean Model and Its Configuration

We use version 3.4 of the Nucleus for European Modeling of Ocean (NEMO) model (Madec, 2012). NEMO solves the incompressible, Boussinesq, hydrostatic, primitive equations on a z coordinate C-grid with a filtered free surface and free-slip lateral boundaries. We use 75 vertical levels, with 24 levels in the first 100 m and 22 levels between 100 and 1,000 m to realistically represent coastlines and continental shelves. Bathymetry is from ETOPO1 (Amante & Eakins, 2009) and is represented by partial cells. NEMO is run with a prognostic turbulent kinetic energy (TKE) scheme for vertical mixing. We use spatially varying lateral eddy coefficients (according to local mesh size) with Laplacian iso-neutral tracer diffusion and biharmonic lateral viscosity.

The model domain is pictured in Figures 1c and 1d. The horizontal grid is curvilinear and eddy permitting (nominally 1/4°; meridional resolution is 24.5 km and zonal resolution is 19.5–24.5 km depending on longitude and latitude). This regional simulation is forced at the open ocean boundaries by temperature, salinity, and velocity 5 day means from a global NEMO ocean simulation run at 1/4° resolution with 75 vertical levels (namely, ORCA025-L75-MJM95, provided by the DRAKKAR/MyOcean group; Barnier et al., 2011). The initial conditions for ocean temperature and salinity are taken from Levitus et al. (1998) with an ocean at rest. River input is prescribed from monthly climatology (Dai & Trenberth, 2002). The regional simulation and ORCA025-L75-MJM95 are both forced at the surface by 10 m winds and 2 m air temperature and humidity (every 3 h) and precipitation, longwave, and shortwave radiation (every day) from the ERA-Interim atmospheric reanalysis (Dee et al., 2011) between 1989 and 2009 through the CORE bulk formulae (Large & Yeager, 2004).

2.2. Experimental Design

Eight experiments are used to investigate the relationship between the EAC separation latitude and the Tasman Sea bathymetry (Figures 1a–1d):

1. *CTRL*: realistic bathymetry (i.e., interpolated from ETOPO1);
2. *noNZ500*: as for CTRL, but New Zealand leveled to 500 m deep (i.e., all bathymetry within the 500 m isobath around NZ, and NZ itself, is set to an ocean depth of 500 m—shaded red in Figure 1b);
3. *FB* ("flat bottom") : bathymetry $>$ 1,000 m deep is set to 4,000 m throughout the domain (apart from near the open boundaries, where bathymetry is linearly interpolated from 4,000 m to ETOPO1 over $\sim$7°). Bathymetry shallower than 1,000 m matches CTRL (note that this includes much of the Campbell Plateau); and

4. *FBnoNZ*: as for FB, but with New Zealand, the Campbell Plateau within the domain and the islands and seamounts between New Zealand and New Caledonia leveled to 4,000 m (retaining New Caledonia as in FB). A small part of Campbell Plateau is retained within the 7° smoothing zone against the southern boundary.

Experiments 5–8 are additional NEMO experiments (CTRL-L, noNZ500-L, FB-L, and FBnoNZ-L) with the same series of bathymetry changes and forcing as in experiments 1–4, but with nonlinear advection terms omitted from the momentum equations; advection is retained in the tracer equations. The southern boundary of the regional domain cuts through Campbell Plateau, so this is only partly removed in experiments 4 and 8.

The CTRL experiment provides a reference of the model's most realistic circulation. The noNZ500 simulation shows the impact of the near-surface New Zealand landmass. The FB and FBnoNZ experiments are designed to be analyzed as a set. The FB experiment is a new control simulation retaining the New Zealand plateau alone, for comparison with its removal in FBnoNZ. To investigate the linear dynamics of the circulation changes due to the removal of New Zealand in the simplest possible scenario, we calculate the steady state Sverdrup/Godfrey Island Rule (Godfrey, 1989; Sverdrup, 1947) stream function (Figures 7a and 7b) with and without New Zealand, utilizing the time-mean ORCA025-L75-MJM95 (global NEMO) wind stress and curl fields. Linear experiments 5–8 extend the Sverdrup balance calculation by including most of the features of experiments 1–4 such as complex bathymetry/continental shelves, stratification (outcropping), and forcing variability.

For the grid points where submarine topography has become part of the ocean domain, Levitus et al. (1998) initial conditions of temperature and salinity are interpolated from the horizontally closest values. Similar island-removing studies by Tilburg et al. (2001) and Penven et al. (2006) do not specify what is done with the atmospheric fluxes over the removed island. In this study, the atmospheric fluxes over the area where New Zealand used to be are the same value as the closest ocean grid point. This removes the effect of New Zealand's orography on local winds and the potential for unrealistic heat fluxes over the ocean grid points coinciding with the New Zealand landmass. We did not attempt to eliminate the effect of NZ on wind stress and other fluxes at the surrounding ocean points. Most importantly, this methodology results in an integrated time-mean wind stress curl that is not significantly different across the experiments, enabling us to test the hypothesis that the partial separation of the EAC is set solely by the meridional gradients in the wind stress curl.

Model outputs and subsequent analyses are based on daily averages. Similar to other boundary current regional configurations (e.g., Renault et al., 2016), all eight NEMO experiments are spun-up for 5 years, and all results in this study use model output between 1 January 1994 and 31 December 2009 (i.e., after the 5 year spin-up phase of 1 January 1989 to 31 December 1993).

3. Model Evaluation

Figure 2 compares the CTRL simulation sea surface height (SSH) to satellite altimetry observations (AVISO) over the years 1994–2009 for which the two products overlap. The time-mean gradients of SSH are generally in good agreement; the EAC and East Auckland Current are clearly visible, and importantly the modeled SSH gradients in the EAC have similar location and structure to the observations. Prior to separation, the upstream EAC has a range of observed and modeled transports from past studies; observed estimates include 27.4 Sv (Ridgway & Godfrey, 1994) and 25.8 Sv (derived from CARS; Ridgway et al., 2002). Modeling estimates of EAC transport range between 20.4 and 30 Sv (Oliver & Holbrook, 2014; Wang et al., 2013; Ypma et al., 2016). In our study, the modeled CTRL upstream EAC transport to 1,945 m across 154°E–156°E at 28°S is 24.3 Sv (Figure 3), and therefore within both modeled and observed estimates of EAC transport, and also consistent with the 22.1 $\pm$ 7.5 Sv directly observed transport at 27°S (Sloyan et al. 2016).

Nonetheless, biases do exist, in the model simulation. For example, there are sharper SSH gradients in CTRL both on the south-eastern side of New Zealand and across the Tasman Sea in the Tasman Front. The bias across the Tasman Sea results in a more focused eastward flow and is typical of other modeling studies in the region (Oliver & Holbrook, 2014; Ypma et al., 2016). The Tasman Front's observed transport is highly variable and at times westward (Sutton & Bowen, 2014). Observed in different time periods, across different sections, mean transport estimates vary: 7.6–8.5 Sv (Stanton, 1979), 12–13 Sv (Stanton, 1981), 12.9 Sv

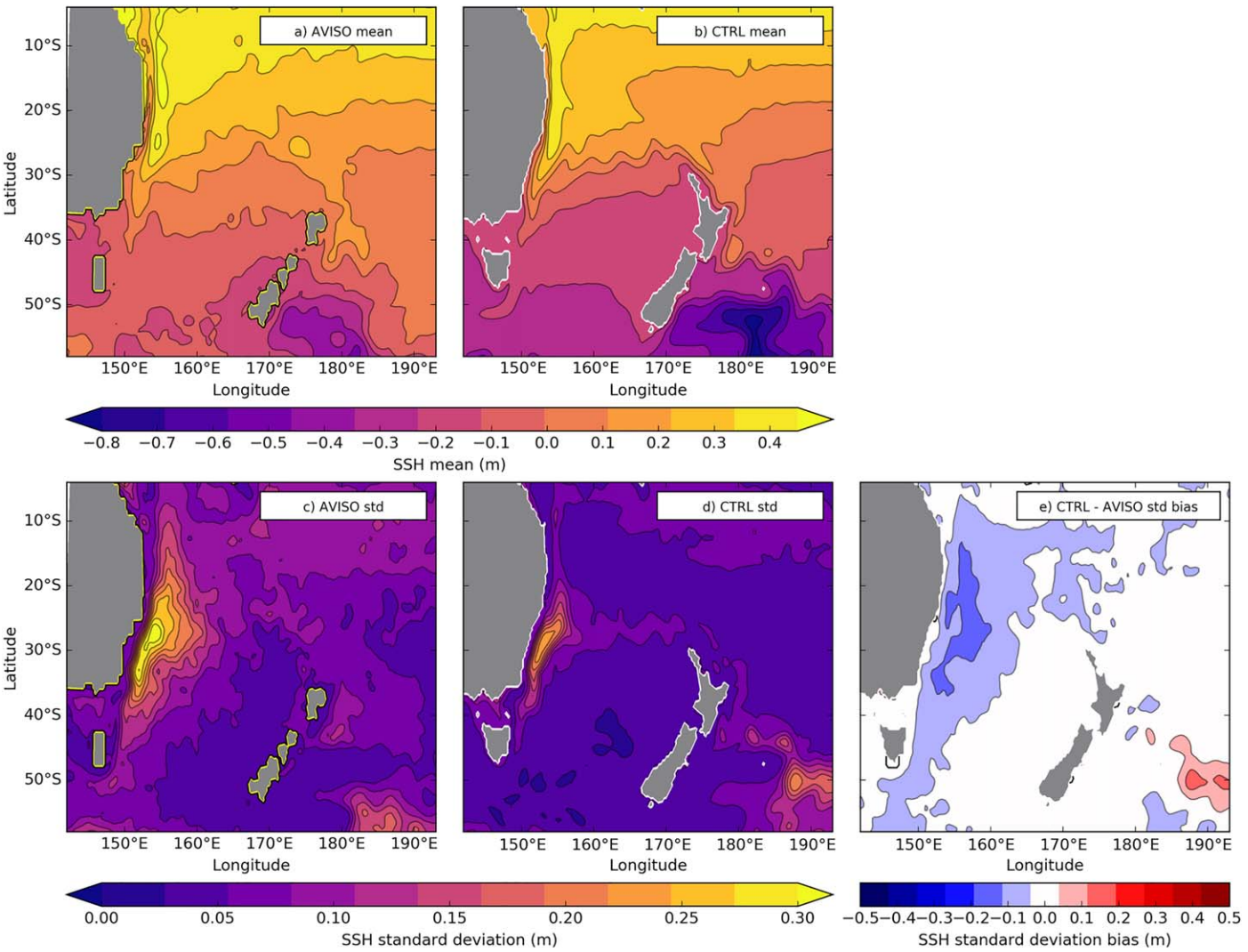

Figure 2. Comparison of NEMO (CTRL) and AVISO sea surface height (SSH) anomaly between 1994 and 2009. (a, b) Mean anomaly and (c–e) standard deviation. The sea surface height mean anomalies are calculated with the temporal and spatial average in the Tasman Sea region removed from the SSH field to emphasize the difference in time-mean gradients between CTRL and AVISO.

(Ridgway & Dunn, 2003), and the first direct measurements by Sutton and Bowen (2014) of 7.8 Sv. The CTRL experiment Tasman Sea mean outflow of 7.6 Sv (Figure 3, section GD) is within the range of observed transports.

The variability of sea surface height in CTRL is also in good agreement with AVISO in many areas but underestimated in the EAC (Figures 2c–2e). This is typical of 1/4° eddy-permitting resolution models (e.g., Ypma et al., 2016). The standard deviation bias (Figure 2e) south-east of New Zealand may be related to the documented semipermanent eddies in the region (see Chiswell & Sutton, 2015, Figure 13), who note that some altimetry data sets do not resolve these features) and/or the strong fronts associated with the confluence of subtropical and subantarctic waters in the region (Fernandez et al., 2014).

4. Results

The importance of New Zealand for the presence and location of the Tasman Front is revealed in Figures 1e–1h by the depth-averaged time-mean kinetic energy field (MKE), defined by $\mathrm{MKE}(x,y) = \frac{\rho_0}{2D}\int_{-D}^{0}(\bar{u}^2(x,y,z) + \bar{v}^2(x,y,z))\,dz$, where $\bar{u}$ and $\bar{v}$ are the time-mean horizontal velocity components, $\rho_0 = 1,035$ kg m^{-3}, and D is

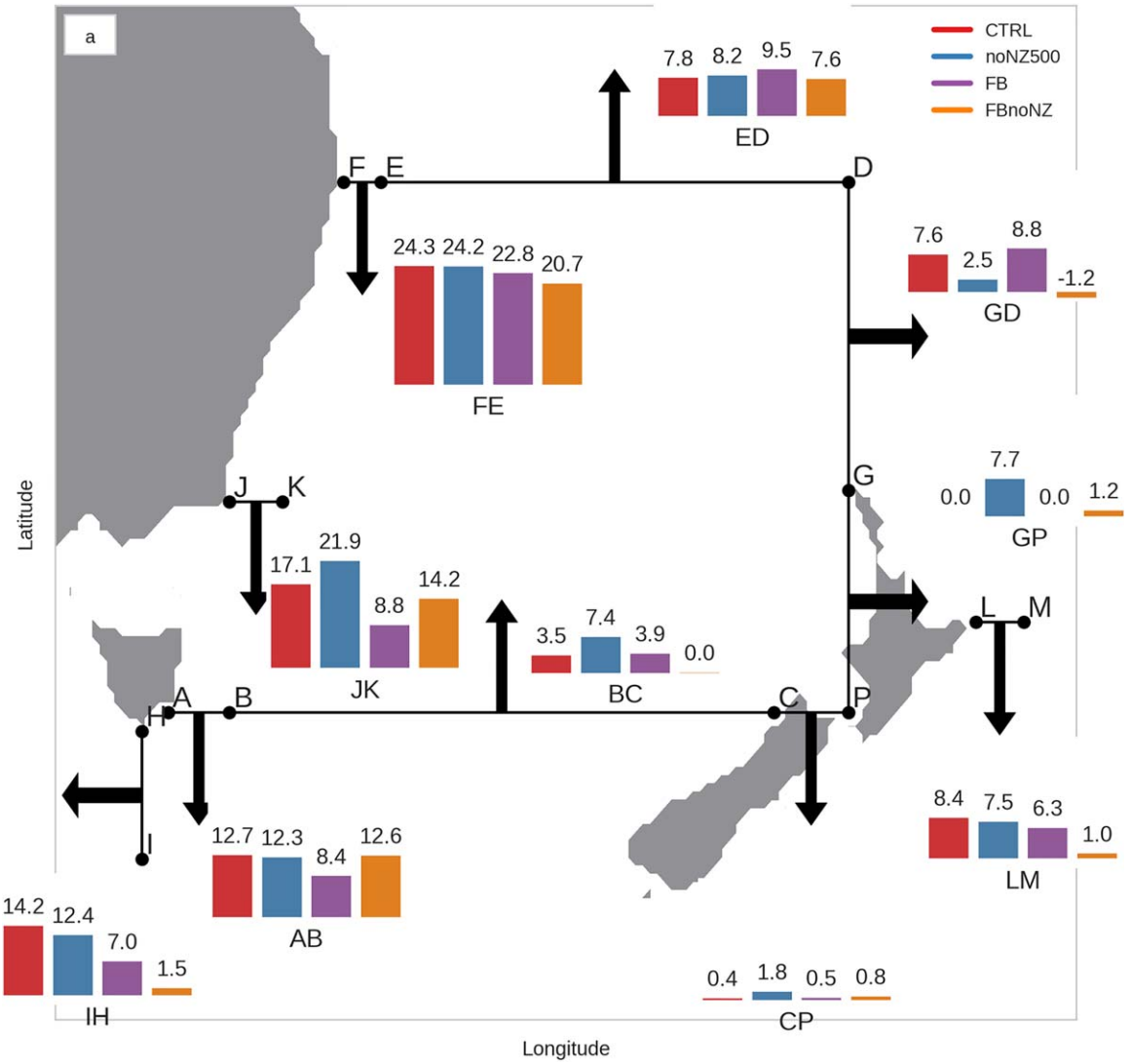

Figure 3. Schematic comparison of depth-integrated transport (Sv) to 1,945 m. Section end points are similar to Oliver and Holbrook (2014) but sections are aligned with the curvilinear model grid (not strictly zonal/meridional); transport is calculated using grid, normal velocities. Section end points are A (148.2°E, 42.6°S), B (150.8°E, 42.6°S), C (172.5°E, 40.6°S), D (171.3°E, 25.8°S), E (155.6°E, 27.6°S), F (153.6°E, 27.8°S), G (173.6°E, 34.9°S), H (146.9°E, 43.4°S), I (146.9°E, 45.8°S), J (150.1°E, 37.1°S), K (151.7°E, 37.1°S), L (178.1°E, 37.5°S), and M (179.9°E, 36.8°S).

the depth of the seafloor or 1,945 m, whichever is shallower. Comparing FB and FBnoNZ in Figures 1g and 1h, the latter has no East Auckland Current/East Cape Current and the partial separation of the EAC has shifted south (barely visible, clearer in Figure 8g). Specifically, FBnoNZ has a much weaker, more zonal Tasman Front located further south, as well as enhanced MKE in the EAC extension. The reduced eastward flow out of the Tasman Sea suggested by Figure 1 is confirmed by the transports shown in Figure 3. The eastward transport north of New Zealand (section GD) decreases from 8.8 to −1.2 Sv when New Zealand is completely removed; FBnoNZ has zero net transport across sections GD + GP. Comparing the EAC extension (JK) with the East Cape Current (LM) sections in Figure 3, from FB to FBnoNZ, the EAC extension (JK) shows an increase of 5.4 Sv which is approximately balanced by a relative reduction of 5.3 Sv in LM. Finally, FBnoNZ shows a large northward shift in the Subantarctic Front (indicated in Figure 1e) south of Australia. This northward shift is associated with the partial removal of Campbell Plateau (compare with noNZ500) and almost completely blocks Tasman Leakage, which drops from 14.2 to 1.5 Sv (section IH).

Compared to CTRL, experiments FB and noNZ500 show much smaller differences than FBnoNZ in Figure 1. Leveling all bathymetry below 1 km to 4 km (FB) leads to a diminished EAC extension and a stronger

recirculation in the separation region. This is consistent with decreased transport in the EAC extension (JK and AB), increased transport offshore flowing north at ED and increased Tasman Front transport (GD; Figure 3). In contrast, leveling the New Zealand landmass to 500 m (noNZ500) leads to a substantial transport increase across BC (3.9 Sv) in the southern Tasman Sea; this is caused by an enhanced northward flow on the western side of the leveled New Zealand landmass (Figure 8c). While Figure 1f suggests noNZ500 has a slightly weaker Tasman Front than CTRL, Figure 3 reveals that the overall Tasman Sea eastward transport (GD + GP) is higher and concentrated further south across GP, and this is compensated by a weaker net southward Tasman Sea outflow (AP) of 6.7 Sv for noNZ500 as compared to 9.6 Sv in the CTRL simulation.

The separation latitude of the EAC shown in Figures 4a–4d is calculated from each daily average snapshot. The separation latitude is found following the method described by Cetina-Heredia et al. (2014) and Ypma et al. (2016), namely, we first find the upstream core of the EAC, defined here as the maximum southward geostrophic surface velocity at 28°S. The SSH contour at the location of the maximum velocity is then followed south and the first location at which the contour turns more than 30° east of south is recorded as the

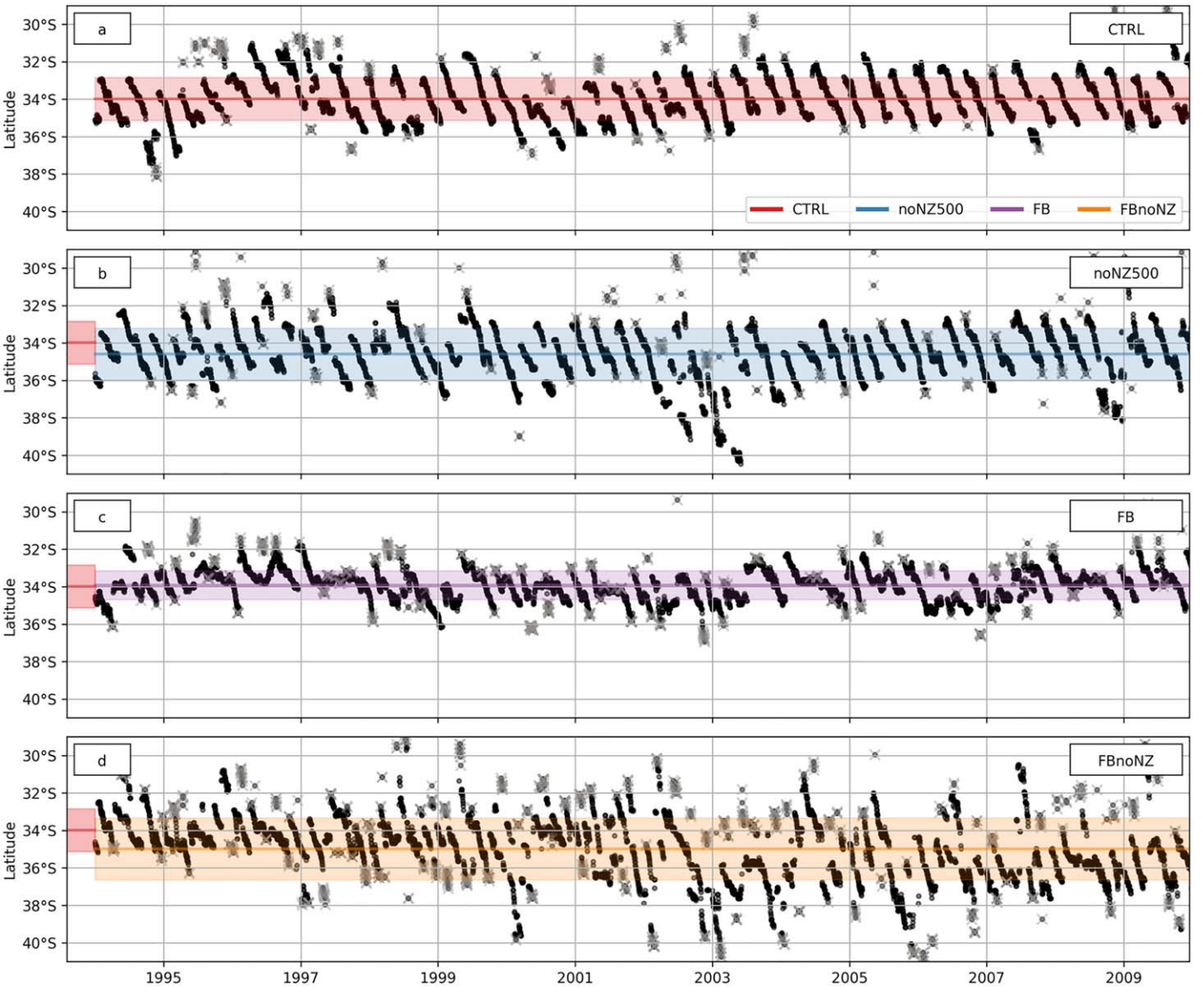

Figure 4. (a–d) Separation latitude time series comparison. Black dots are detected separation latitude (gray crosses are false-positive outputs by the separation latitude algorithm). Thick solid line indicates the mean of each experiment and the shaded region indicates one standard deviation. CTRL mean and standard deviation are shown in Figures 4b–4d to highlight changes from CTRL.

separation latitude. In summary, the time series describes where a representative EAC SSH contour first separates from the coast. Each diagonal line segment in the CTRL simulation (Figure 4a) represents the growth of the EAC retroflection south, then at ~35°S–37°S the detected EAC separation latitude retracts abruptly north to ~33°S (where the black line segment has a discontinuity). This occurs when an eddy detaches from the EAC, producing a closed SSH contour so that the detected separation latitude jumps from the southern to the northern edge of the eddy as it is shed. Therefore, the mean of the separation latitude (thick red line) is not the mean latitude at which eddies are shed (~33°S). Consistent with the flat-bottom experiment of Tilburg et al. (2001), experiment FB's mean separation is essentially unchanged (northward shift of 0.1°, Figure 4c), however, the standard deviation is reduced by 32%. Removal of New Zealand causes a 0.6° southward shift of the mean separation latitude in noNZ500 relative to CTRL (Figures 4a and 4b); for comparison, Tilburg et al. (2001) have a negligible shift in EAC separation on removal of New Zealand in their linear 1.5-layer experiments with an active layer thickness of 250 m. A much stronger contrast to Tilburg et al. (2001) is seen in the difference between FB and FBnoNZ (Figures 4c and 4d) which shows that the removal of New Zealand shifts the mean separation latitude 1.1° further south, and also produces a much less organized pattern of eddy shedding in both timing and latitude, doubling the standard deviation of the separation latitude from 0.8° to 1.6°. The first minimum in the separation latitude autocorrelation across all experiments occurs within 120 days. Taking 120 days as a conservative interval for independent samples yields a maximum standard error in the mean EAC separation latitude of 0.1° and 0.2° for FB and FBnoNZ, respectively. The 1.1° shift in the mean between FB and FBnoNZ is therefore statistically significant, despite being within the typical range of an individual eddy-shedding cycle. The 1.1° shift in the mean is also larger than those reported in both recent (1980–2010) and future climate simulations (Cetina-Heredia et al., 2014; Oliver & Holbrook, 2014, respectively).

To summarize, when New Zealand is completely removed (FBnoNZ), the EAC's eddies travel a greater distance south before separating from the main current, but the EAC retracts to a similar latitude after eddy separation, giving a larger range of latitudes. Thus, the shift in MKE (Figures 1g and 1h) between FB and FBnoNZ is due to the EAC separation transiently reaching farther south in FBnoNZ (Figure 4). This result, along with the change in Tasman Front position as shown in MKE in Figure 1, forms the evidence for the main finding of this paper: that bathymetric features around New Zealand play a key role in reducing the southward penetration of the EAC extension, which in turn causes the time-mean partial separation of the EAC to be 1.1° further north than it would be in the absence of New Zealand.

We now focus on the largest changes between the experiments, namely between FB and FBnoNZ (with and without New Zealand where all bathymetry below 1km is leveled to 4 km, respectively). The SSH variability changes shown in Figure 5 corroborate the former discussion around the Tasman Sea circulation changes

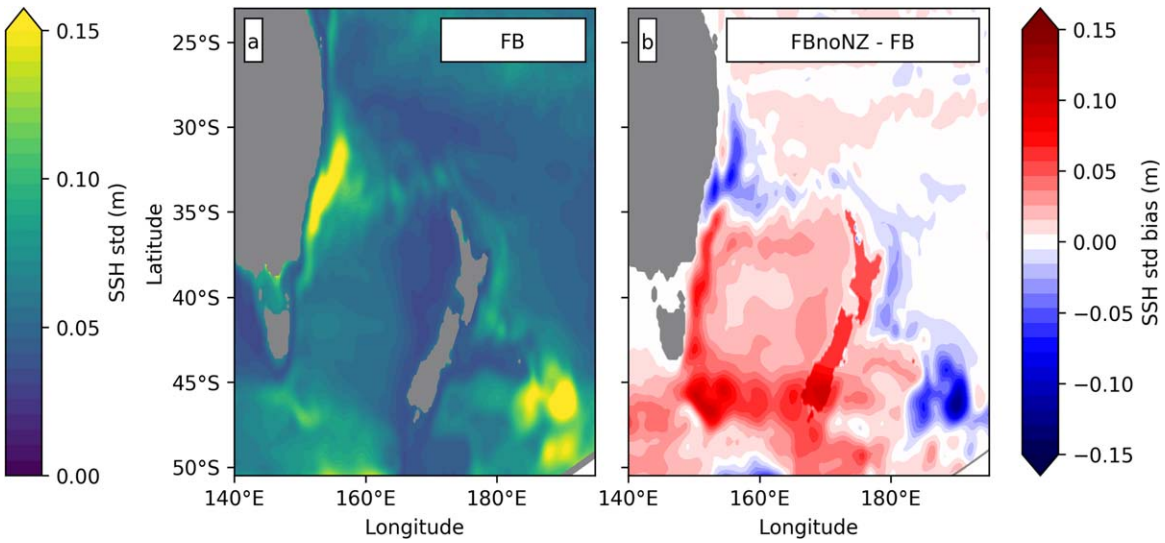

Figure 5. (a) Standard deviation of sea surface height (m) for FB. (b) Sea surface height standard deviation difference (m) between FB and FBnoNZ. Red (blue) indicates increased (decreased) variability in FBnonNZ.

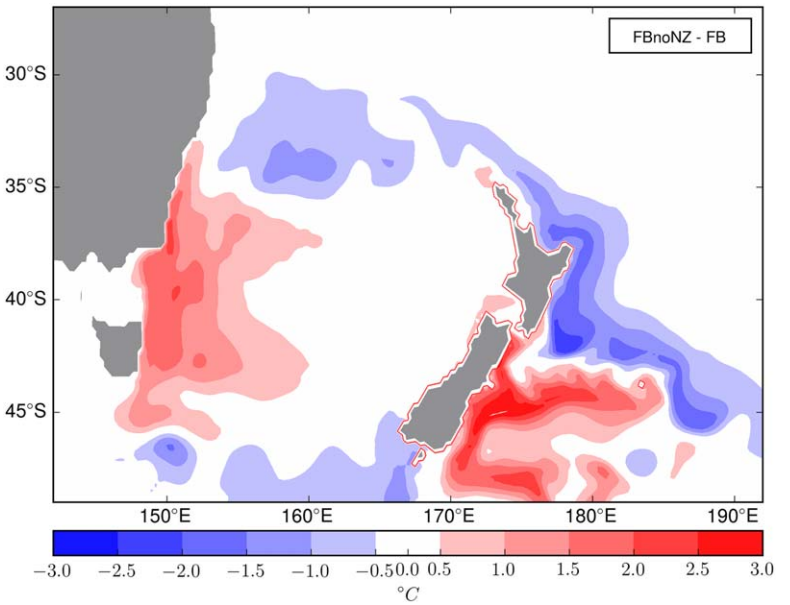

Figure 6. Time-mean sea surface temperature difference between FB and FBnoNZ.

shown in Figures 1, 3, and 4. Specifically, FBnoNZ has reduced variability in the separation region, Tasman Front and East Auckland Current but enhanced variability in the southern half of the Tasman Sea and south of Tasmania. The circulation changes between experiments FB and FBnoNZ demonstrate the importance of the New Zealand submarine platform in setting the spatial structure of temperature in the Tasman Sea as shown in Figure 6. The greater southward migration of EAC extension eddies in FBnoNZ, as compared to FB (discussed in Figure 4 and also visible in Figure 5) leads to a warming of ∼2°C in the EAC extension region. Due to the change in the EAC's partial separation and weakening of the Tasman Front (see Figures 1g and 1h), there is a similar reduction in temperature across the Tasman Sea and the East Auckland Current. The warming on the south-eastern side of New Zealand on partial removal of Campbell Plateau is due to the elimination of topographic steering, which normally directs cold Subantarctic waters northward.

Barotropic stream functions for different model parameters are shown in Figures 7 and 8 to investigate the dynamical reasons for the changes in Tasman Front position and EAC separation latitude. The Sverdrup/

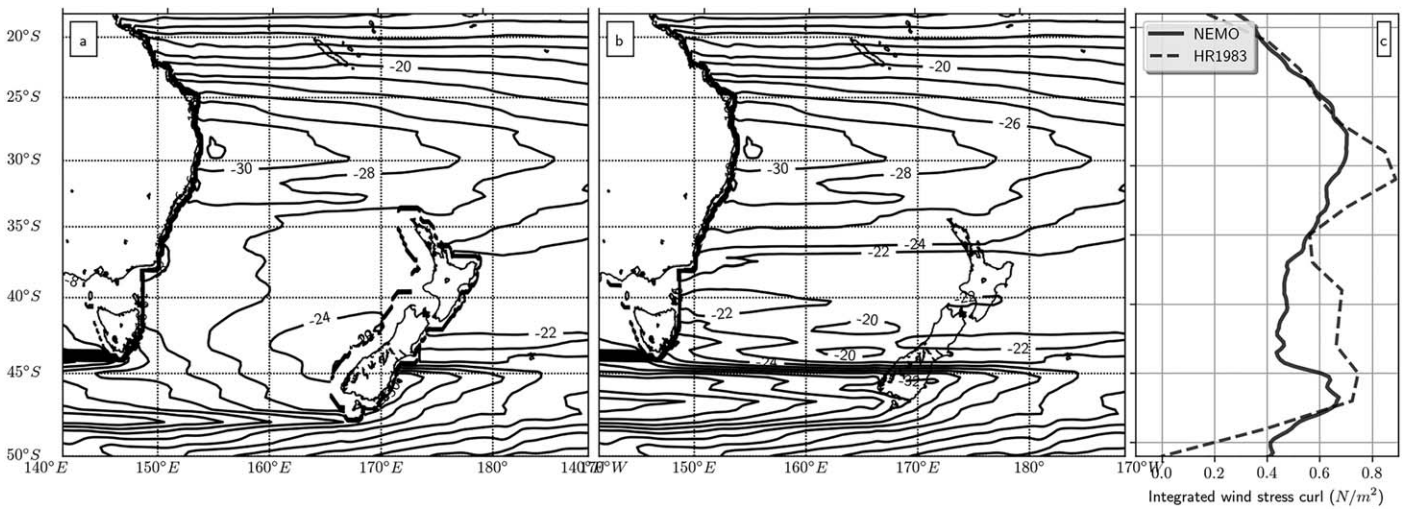

Figure 7. Analytical Godfrey Island Rule stream function (a) with and (b) without New Zealand; contours every 2 Sv. Wind stress and curl fields are from NEMO (time-mean ERA-Interim atmospheric reanalysis as felt by ORCA025-L75-MJM95; over New Zealand in Figures 7b and 7c the wind stress curl is zero). (c) Time-mean zonally integrated South Pacific (145°E–291°E) wind stress curl from NEMO and Hellerman and Rosenstein (1983).

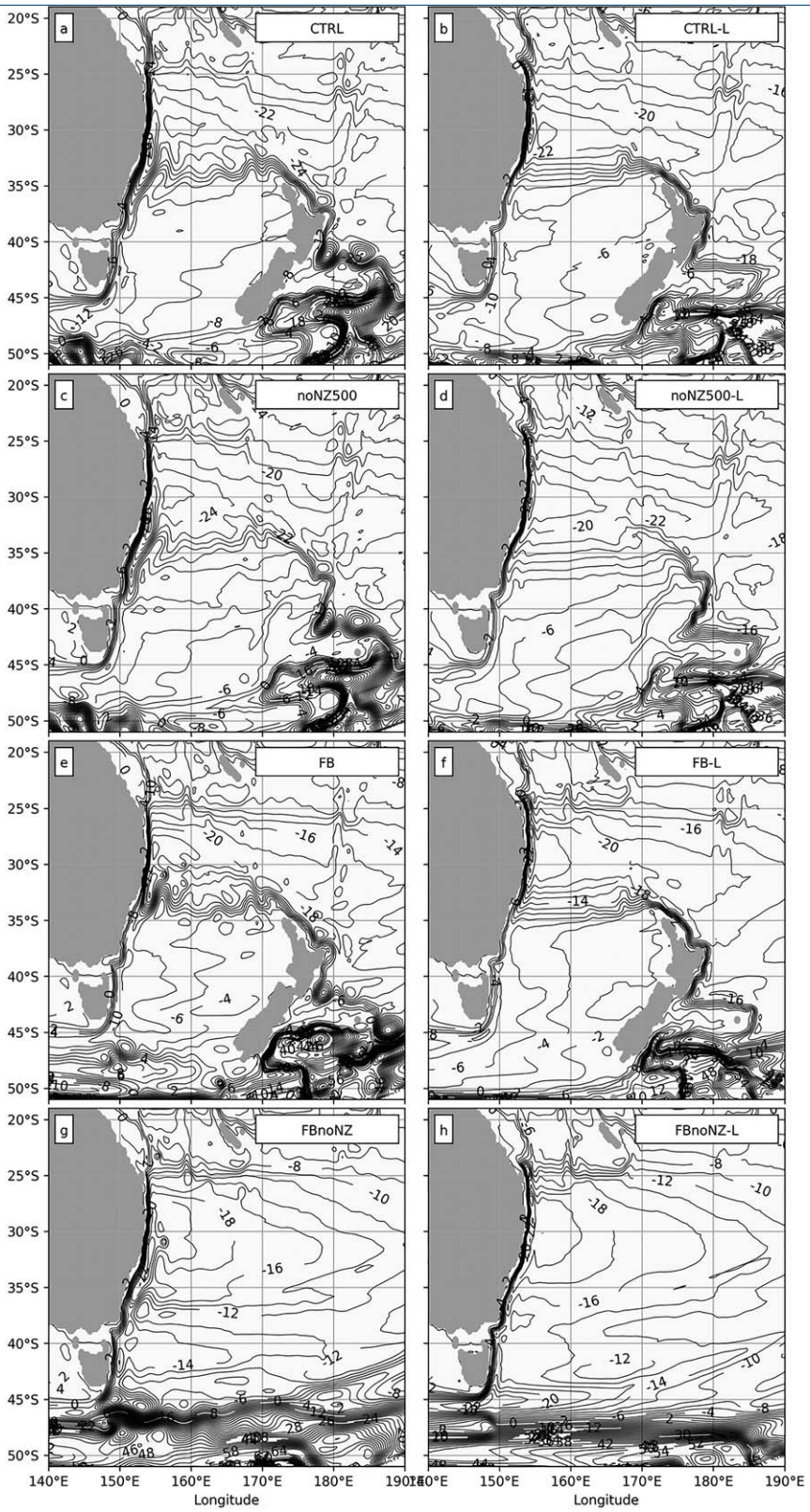

Figure 8. (a–h) Time-mean barotropic stream function comparison (integration taken eastward from Australia down to 1,945 m; contours every 2 Sv) for perturbed bathymetry NEMO experiments. (left) Nonlinear experiments and (right) linear or "−L" experiments; see section 2.2 for experiment details.

Island Rule stream function in Figures 7a and 7b illustrates the importance of New Zealand in setting the time-mean location of the EAC outflow under ERA-Interim forcing. Comparing Figure 7a with Figure 7b, when the New Zealand coastline is removed, the outflow is no longer constrained by the northern tip of New Zealand. This southward shift in the position of the Tasman Sea outflow was not seen in the Tilburg et al. (2001) solution and is likely caused by different meridional gradients in the wind stress curl products shown in Figure 7c (further discussed in section 5).

In the Tilburg et al. (2001) RG1/RG2 simulations, the authors inferred that nonlinearities were unimportant for setting the time-mean EAC separation; this issue is now revisited. Figure 8 examines the importance of nonlinear processes by comparing NEMO experiments with (left column) and without (right column) the nonlinear advection terms in the momentum calculation. These experiments extend the 1.5-layer linear experiments RG1 and RG2 of Tilburg et al. (2001) by including continental shelves, stratification, and topographic steering. Consistent with Ridgway & Godfrey (1994) and Tilburg et al. (2001), circulation features that are reliant on eddies (for example, the mean EAC retroflection or eddy driven recirculation at ~32°S in Figure 8e) are not present in the linear simulation (FB-L in Figure 8f). On the gyre scale, the inclusion of momentum advection (Figures 8a, 8c, 8e, and 8g) breaks the north-south symmetry of the gyre, leading to downstream intensification of the EAC (compare Figures 8g and 8h). Away from the western boundary, the effects of changing topography on the mean Tasman Front are similar in the linear and nonlinear experiments. The linear experiments in Figures 8b, 8d, and 8f show a similar, narrow Tasman Front when New Zealand or the subsurface New Zealand landmass is present (slightly broader in noNZ500-L), whereas the complete removal of New Zealand leads to a broader outflow than in the nonlinear case (Figures 8g and 8h). In summary, the presence of the New Zealand submarine platform is crucial to maintaining a narrow, coherent current across the northern Tasman Sea, and nonlinearity is important in controlling the extent of the retroflection in the EAC extension.

5. Discussion and Conclusions

Using a suite of modified bathymetry NEMO ocean model experiments, we have found that the complete removal of New Zealand leads to broader offshore flow (formerly the Tasman Front) and an EAC extension that extends further south. These experiments challenge the conventional view that the EAC's partial separation is set by the wind field alone (Ridgway & Dunn, 2003; Tilburg et al., 2001). Due to the small surface area where New Zealand is removed and the minor effect of relative wind (Dawe & Thompson, 2006), the CTRL and FBnoNZ experiments are driven by nearly the same time-mean integrated wind stress curl. Since FB and FBnoNZ show different EAC partial separation behavior, these results show that the steepest gradient in the basin-averaged wind stress curl is not the sole factor determining the latitude of partial separation of the EAC. This is an important consideration for attribution studies (e.g., Feng et al., 2016; Oliver & Holbrook, 2014) that relate changes in circulation to changes in the wind stress curl.

Tilburg et al. (2001)'s analysis of the removal of New Zealand was limited in a number of ways. First, their 1.5-layer model represented landmasses by their 250 m isobath and could not address the effect of removing subsurface features such as shelves and ridges. Second, their East Auckland Current flowed north (the wrong direction) and lastly, the model they used did not incorporate higher vertical modes, isopycnal outcropping or nonlinear dynamics (vorticity advection and flow instabilities). The NEMO model solutions address many of these deficiencies, particularly the role of subsurface bathymetry. We found that the mean flow in the linear NEMO model experiments is qualitatively consistent with the full NEMO solutions, with the main exception that nonlinearity affects the extent of the mean retroflection in the EAC extension. We infer that deep bathymetry plays a major role in forming a narrow Tasman Front and nonlinear processes (e.g., eddies, rectification, and momentum advection) are crucial for the extent of the EAC retroflection.

We find that removal of New Zealand affects the Tasman Front latitude in our linear and nonlinear experiments, in contrast to the linear experiments of Tilburg et al. (2001). We attribute this difference to our use of the ERA-Interim wind stress product which is a significant improvement on the Hellerman and Rosenstein (1983) product used by Tilburg et al. (2001), as it is based on ERS-1, ERS-2, and QuickSCAT satellite coverage between 1992 and 2009 (Dee et al., 2011). In particular, the Hellerman and Rosenstein (1983) integrated wind stress curl drops steeply from 30°S to 35°S (north of New Zealand) but falls more gradually between 29°S and 42°S in ERA-Interim (Figure 7c). Sverdrup dynamics dictate a strong outflow from the EAC in the

region of strong wind stress curl gradient, explaining why Tilburg et al. (2001) found little effect of New Zealand on the Tasman Front (or EAC separation) latitude. In contrast, our Sverdrup/Godfrey Island Rule calculation with ERA-Interim (Figure 7) shows that the outflow location moves south when New Zealand is removed. Features obviously related to topography and nonlinearity aside, linear and nonlinear NEMO experiments show the same effect (Figure 8). We conclude that when New Zealand is absent, the maximum wind stress curl gradient sets the Tasman Front latitude but if New Zealand is present then the latitude of maximum wind stress curl gradient sets the Tasman Front location if it is north of New Zealand, but otherwise New Zealand sets the Tasman Front location.

The time scales, resolution dependence and dynamics that determine the EAC partitioning between the EAC extension and Tasman Front remain an interesting topic that requires further investigation. Improving our understanding of the EAC dynamics controlling the separation is a key step toward quantifying climate change driven impacts on regional circulation and marine ecosystems. While this study has shown that New Zealand affects the position of the EAC separation and Tasman Front under 1989–2009 ERA-Interim forcing, the degree to which this relationship persists under anthropogenic changes to the wind stress curl is an open question. Future work could perturb the wind field in a realistic way and look at changes in Tasman Sea circulation with respect to response times and sensitivity (e.g., Durgadoo et al., 2013). Coarse-resolution (1° at 30°S) modeling results suggest that the Tasman Front transport is correlated to EAC transport (Sloyan & O'Kane, 2015); analogous results in the Agulhas system however have shown that decoupling between the Agulhas current and Agulhas leakage occurs at higher resolutions (Holton et al., 2016; Loveday et al., 2014). Hence, future work is best completed with eddy-resolving resolution in which the wind field is perturbed in isolation.

Acknowledgments

The altimeter products were produced by Ssalto/Duacs and distributed by Aviso with support from Cnes. The AVISO product used is the daily, delayed time, all satellite, Mapped Absolute Dynamic Topography (DT-MADT) product consisting of the mean dynamic topography from MDT CNES-CLS13 (Rio et al., 2014) and Mapped Sea Level Anomalies from DUACS DT2014 (Pujol et al., 2016). This work was supported by an Australian Government Research Training Program Scholarship and the Australian Research Council (ARC), specifically, the ARC Centre of Excellence in Climate System Science (CE110001028) and grant DE130101336. This research was undertaken with the assistance of resources from the National Computational Infrastructure (NCI), which is supported by the Australian Government. All model output generated in this study is archived in the UNSW Data Archive. We are grateful to Eric C. J. Oliver for providing the Godfrey Island Rule analysis code. We thank Gurvan Madec for his NEMO expertise and suggestions on how to improve the manuscript.

References

Amante, C., & Eakins, B. W. (2009). *ETOPO1 1 arc-minute global relief model: Procedures, data sources and analysis* (NOAA Tech. Memo. NESDIS NGDC-24). Retrieved from https://doi.org/10.1594/PANGAEA.769615

Andrews, J. C., & Scully-Power, P. (1976). The structure of an East Australian Current anticyclonic eddy. *Journal of Physical Oceanography*, *6*, 756–765.

Barnier, B., Dussin, R., & Molines, J. M. (2011). *Scientific Validation Report (ScVR) for V1 reprocessed analysis and reanalysis* (Rep. WP 04-GLO-CNRS_LEGI Grenoble).

Bostock, H. C., Opdyke, B. N., Gagan, M. K., Kiss, A. E., & Fifield, L. K. (2006). Glacial/interglacial changes in the East Australian Current. *Climate Dynamics*, *26*(6), 645–659. https://doi.org/10.1007/s00382-005-0103-7

Cai, W. (2006). Antarctic ozone depletion causes an intensification of the Southern Ocean super-gyre circulation. *Geophysical Research Letters*, *33*, L03712. https://doi.org/10.1029/2005GL024911

Cai, W., Shi, G., Cowan, T., Bi, D., & Ribbe, J. (2005). The response of the Southern Annular Mode, the East Australian Current, and the southern mid-latitude ocean circulation to global warming. *Geophysical Research Letters*, *32*, L23706. https://doi.org/10.1029/2005GL024701

Cetina-Heredia, P., Roughan, M., van Sebille, E., & Coleman, M. A. (2014). Long-term trends in the East Australian Current separation latitude and eddy driven transport. *Journal of Geophysical Research: Oceans*, *119*, 4351–4366. https://doi.org/10.1002/2014JC010071

Chiswell, S. M., Bostock, H. C., Sutton, P. J., & Williams, M. J. (2015). Physical oceanography of the deep seas around New Zealand: A review. *New Zealand Journal of Marine and Freshwater Research*, *8330*, 1–32. https://doi.org/10.1080/00288330.2014.992918

Chiswell, S. M., & Sutton, P. J. (2015). Drifter- and float-derived mean circulation at the surface and 1000 m in the New Zealand region. *New Zealand Journal of Marine and Freshwater Research*, *49*(2), 259–277. https://doi.org/10.1080/00288330.2015.1008522

Couvelard, X., Marchesiello, P., Gourdeau, L., & Lefèvre, J. (2008). Barotropic zonal jets induced by islands in the Southwest Pacific. *Journal of Physical Oceanography*, *38*(10), 2185–2204. https://doi.org/10.1175/2008JPO3903.1

Dai, A., & Trenberth, K. E. (2002). Estimates of freshwater discharge from continents: Latitudinal and seasonal variations. *Journal of Hydrometeorology*, *3*(6), 660–687. https://doi.org/10.1175/1525-7541(2002)003<0660:EOFDFC>2.0.CO;2

Dawe, J. T., & Thompson, L. A. (2006). Effect of ocean surface currents on wind stress, heat flux, and wind power input to the ocean. *Geophysical Research Letters*, *33*, L09604. https://doi.org/10.1029/2006GL025784

Dee, D. P., Uppala, S. M., Simmons, A. J., Berrisford, P., Poli, P., Kobayashi, S., et al. (2011). The ERA-Interim reanalysis: Configuration and performance of the data assimilation system. *Quarterly Journal of the Royal Meteorological Society*, *137*(656), 553–597. https://doi.org/10.1002/qj.828

Durgadoo, J. V., Loveday, B. R., Reason, C. J. C., Penven, P., & Biastoch, A. (2013). Agulhas leakage predominantly responds to the Southern Hemisphere westerlies. *Journal of Physical Oceanography*, *43*(10), 2113–2131. https://doi.org/10.1175/JPO-D-13-047.1

Everett, J. D., Baird, M. E., Oke, P. R., & Suthers, I. M. (2012). An avenue of eddies: Quantifying the biophysical properties of mesoscale eddies in the Tasman Sea. *Geophysical Research Letters*, *39*, L16608. https://doi.org/10.1029/2012GL053091

Feng, M., Zhang, X., Oke, P., Monselesan, D., Chamberlain, M., Matear, R., et al. (2016). Invigorating ocean boundary current systems around Australia during 1979–2014: As simulated in a near-global eddy-resolving ocean model. *Journal of Geophysical Research: Oceans*, *121*, 3395–3408. https://doi.org/10.1002/2016JC011842

Fernandez, D., Bowen, M., & Carter, L. (2014). Intensification and variability of the confluence of subtropical and subantarctic boundary currents east of New Zealand. *Journal of Geophysical Research: Oceans*, *119*, 1146–1160. https://doi.org/10.1002/2013JC009153

Godfrey, J. S. (1989). A Sverdrup model of the depth-integrated flow for the world ocean allowing for island circulations. *Geophysical & Astrophysical Fluid Dynamics*, *45*(1–2), 89–112. https://doi.org/10.1080/03091928908208894

Godfrey, J. S., Cresswell, G. R., Golding, T. J., Pearce, A. F., & Boyd, R. (1980). The separation of the East Australian Current. *Journal of Physical Oceanography*, *10*(3), 430–440. https://doi.org/10.1175/1520-0485(1980)010<0430:TSOTEA>2.0.CO;2

Gray, A. R., & Riser, S. C. (2014). A global analysis of Sverdrup balance using absolute geostrophic velocities from Argo. *Journal of Physical Oceanography*, *44*(4), 1213–1229. https://doi.org/10.1175/JPO-D-12-0206.1

Heath, R. A. (1985). Large-scale influence of the New Zealand seafloor topography on western boundary currents of the South Pacific Ocean. *Australian Journal of Marine and Freshwater Research*, *36*, 1–14. https://doi.org/10.1071/MF9850001

Hellerman, S., & Rosenstein, M. (1983). Normal monthly wind stress over the world ocean with error estimates. *Journal of Physical Oceanography*, *13*(7), 1093–1104. https://doi.org/10.1175/1520-0485(1983)013<1093:NMWSOT>2.0.CO;2

Hill, K. L., Rintoul, S. R., Ridgway, K. R., & Oke, P. R. (2011). Decadal changes in the South Pacific western boundary current system revealed in observations and ocean state estimates. *Journal of Geophysical Research*, *116*, C01009. https://doi.org/10.1029/2009JC005926

Holton, L., Deshayes, J., Backeberg, B. C., Loveday, B. R., Hermes, J. C., & Reason, C. J. C. (2016). Spatio-temporal characteristics of Agulhas leakage: A model inter-comparison study. *Climate Dynamics*, *48*(7), 1–15. https://doi.org/10.1007/s00382-016-3193-5

Hu, D., Wu, L., Cai, W., Sen Gupta, A., Ganachaud, A., Qiu, B., et al. (2015). Pacific western boundary currents and their roles in climate. *Nature*, *522*(7556), 299–308. https://doi.org/10.1038/nature14504

Large, W. G., & Yeager, S. G. (2004). *Diurnal to decadal global forcing for ocean and sea–ice models: The data sets and flux climatologies* (NCAR Tech. Note TN-460+ST, 105 pp.). Retrieved from https://doi.org/10.5065/D6KK98Q6

Levitus, S., Conkright, M., Boyer, T., O'Brien, T., Antonov, J., Stephens, C., et al. (1998). World ocean database 1998, volume 1: Introduction. In *NOAA Atlas NESDIS 18* (346 pp.). Washington, DC: United States Government Publishing Office.

Loveday, B. R., Durgadoo, J. V., Reason, C. J. C., Biastoch, A., & Penven, P. (2014). Decoupling of the Agulhas leakage from the Agulhas Current. *Journal of Physical Oceanography*, *44*, 140411151744003. https://doi.org/10.1175/JPO-D-13-093.1

Madec, G. (2012). *NEMO ocean engine* (*Note du Pôle modélisation*, Vol. 27, 357 pp.). Institute Pierre Simon Laplace.

Mata, M. M., Wijffels, S. E., Church, J. A., & Tomczak, M. (2006). Eddy shedding and energy conversions in the East Australian Current. *Journal of Geophysical Research*, *111*, C09034. https://doi.org/10.1029/2006JC003592

Munk, W. H. (1950). On the wind-driven ocean circulation. *Journal of Meteorology*, *7*(2), 80–93.

Nilsson, C. S., & Cresswell, G. R. (1980). The formation and evolution of East Australian Current warm-core eddies. *Progress in Oceanography*, *9*(3), 133–183. https://doi.org/10.1016/0079-6611(80)90008-7

Oliver, E. C. J., & Holbrook, N. J. (2014). Extending our understanding of South Pacific gyre "spin-up": Modeling the East Australian Current in a future climate. *Journal of Geophysical Research: Oceans*, *119*, 2788–2805. https://doi.org/10.1002/2013JC009591

Pedlosky, J. (1996). *Ocean circulation theory*. Berlin, Germany: Springer.

Penven, P., Lutjeharms, J. R. E., & Florenchie, P. (2006). Madagascar: A pacemaker for the Agulhas Current system? *Geophysical Research Letters*, *33*, L17609. https://doi.org/10.1029/2006GL026854

Pilo, G. S., Oke, P. R., Rykova, T., Coleman, R., & Ridgway, K. (2015). Do East Australian Current anticyclonic eddies leave the Tasman Sea? *Journal of Geophysical Research: Oceans*, *120*, 8099–8114. https://doi.org/10.1002/2015JC011026

Pujol, M. I., Faugère, Y., Taburet, G., Dupuy, S., Pelloquin, C., Ablain, M., et al. (2016). DUACS DT2014: The new multi-mission altimeter data set reprocessed over 20 years. *Ocean Science*, *12*(5), 1067–1090. https://doi.org/10.5194/os-12-1067-2016

Renault, L., Molemaker, M. J., McWilliams, J. C., Shchepetkin, A. F., Lemarié, F., Chelton, D., et al. (2016). Modulation of wind work by oceanic current interaction with the atmosphere. *Journal of Climate*, *46*, 1685–1704. https://doi.org/10.1175/JPO-D-15-0232.1

Ridgway, K., & Dunn, J. (2003). Mesoscale structure of the mean East Australian Current System and its relationship with topography. *Progress in Oceanography*, *56*(2), 189–222. https://doi.org/10.1016/S0079-6611(03)00004-1

Ridgway, K., Dunn, J. R., & Wilkin, J. L. (2002). Ocean interpolation by four-dimensional weighted least squares—Application to the waters around Australasia. *Journal of Atmospheric and Oceanic Technology*, *19*(9), 1357–1375.

Ridgway, K. R. (2007). Long-term trend and decadal variability of the southward penetration of the East Australian Current. *Geophysical Research Letters*, *34*, L13613. https://doi.org/10.1029/2007GL030393

Ridgway, K. R., Coleman, R. C., Bailey, R. J., & Sutton, P. (2008). Decadal variability of East Australian Current transport inferred from repeated high-density XBT transects, a CTD survey and satellite altimetry. *Journal of Geophysical Research*, *113*, C08039. https://doi.org/10.1029/2007JC004664

Ridgway, K. R., & Dunn, J. R. (2007). Observational evidence for a Southern Hemisphere oceanic supergyre. *Geophysical Research Letters*, *34*, L13612. https://doi.org/10.1029/2007GL030392

Ridgway, K. R., & Godfrey, J. S. (1994). Mass and heat budgets in the East Australian Current: A direct approach. *Journal of Geophysical Research*, *99*, 3231–3248.

Rio, M. H., Mulet, S., & Picot, N. (2014). Beyond GOCE for the ocean circulation estimate: Synergetic use of altimetry, gravimetry, and in situ data provides new insight into geostrophic and Ekman currents. *Geophysical Research Letters*, *41*, 8918–8925. https://doi.org/10.1002/2014GL061773

Roemmich, D., Gilson, J., Sutton, P., & Zilberman, N. (2016). Multidecadal change of the South Pacific gyre circulation. *Journal of Physical Oceanography*, *46*(6), 1871–1883. https://doi.org/10.1175/JPO-D-15-0237.1

Sen Gupta, A., McGregor, S., van Sebille, E., Ganachaud, A., Brown, J., & Santoso, A. (2016). Future changes to the Indonesian Throughflow and Pacific circulation: The differing role of wind and deep circulation changes. *Geophysical Research Letters*, *43*, 1669–1678. https://doi.org/10.1002/2016GL067757

Sloyan, B. M., & O'Kane, T. J. (2015). Drivers of decadal variability in the Tasman Sea. *Journal of Geophysical Research: Oceans*, *120*, 3193–3210. https://doi.org/10.1002/2014JC010550

Sloyan, B. M., Ridgway, K. R., & Cowley, R. (2016). The East Australian Current and property transport at 27°S from 2012–2013. *Journal of Physical Oceanography*, *46*, 993–1008. https://doi.org/10.1175/JPO-D-15-0052.1

Speich, S., Blanke, B., & Cai, W. (2007). Atlantic meridional overturning circulation and the Southern Hemisphere supergyre. *Geophysical Research Letters*, *34*, L23614. https://doi.org/10.1029/2007GL031583

Stanton, B. R. (1979). The Tasman Front. *New Zealand Journal of Marine and Freshwater Research*, *13*(2), 201–214. https://doi.org/10.1080/00288330.1979.9515795

Stanton, B. R. (1981). An oceanographic survey of the Tasman Front. *New Zealand Journal of Marine and Freshwater Research*, *15*(3), 289–297. https://doi.org/10.1080/00288330.1981.9515924

Sutton, P. J. H., & Bowen, M. (2014). Flows in the Tasman Front south of Norfolk Island. *Journal of Geophysical Research: Oceans*, *119*, 3041–3053. https://doi.org/10.1002/2013JC009543

Sverdrup, H. U. (1947). Wind-driven currents in a Baroclinic Ocean; with application to the equatorial currents of the Eastern Pacific. *Proceedings of the National Academy of Sciences of the United States of America*, *33*(11), 318–326.

Swart, N. C., & Fyfe, J. C. (2012). Observed and simulated changes in the Southern Hemisphere surface westerly wind-stress. *Geophysical Research Letters*, *39*, L16711. https://doi.org/10.1029/2012GL052810

Thomas, M. D., De Boer, A. M., Johnson, H. L., & Stevens, D. P. (2014). Spatial and temporal scales of Sverdrup balance. *Journal of Physical Oceanography*, *44*(10), 2644–2660. https://doi.org/10.1175/JPO-D-13-0192.1

Tilburg, C. E., Hurlburt, H. E., O'Brien, J. J., & Shriver, J. F. (2001). The dynamics of the East Australian Current System: The Tasman Front, the East Auckland Current, and the East Cape Current. *Journal of Physical Oceanography*, *31*(10), 2917–2943. https://doi.org/10.1175/1520-0485(2001)031<2917:TDOTEA>2.0.CO;2

van Sebille, E., England, M. H., Zika, J. D., & Sloyan, B. M. (2012). Tasman Leakage in a fine-resolution ocean model. *Geophysical Research Letters*, *39*, L06601. https://doi.org/10.1029/2012GL051004

Wang, X. H., Bhatt, V., & Sun, Y.-J. (2013). Study of seasonal variability and heat budget of the East Australian Current using two eddy-resolving ocean circulation models. *Ocean Dynamics*, *63*(5), 549–563. https://doi.org/10.1007/s10236-013-0605-5

Warren, B. A. (1970). General circulation in the South Pacific. In W. S. Wooster (Ed.), *Scientific exploration of the South Pacific* (pp. 33–49). Washington, DC: National Academy of Sciences.

Wu, L., Cai, W., Zhang, L., Nakamura, H., Timmermann, A., Joyce, T., et al. (2012). Enhanced warming over the global subtropical western boundary currents. *Nature Climate Change*, *2*(3), 161–166. https://doi.org/10.1038/nclimate1353

Yang, H., Lohmann, G., Wei, W., Dima, M., Ionita, M., & Liu, J. (2016). Intensification and poleward shift of subtropical western boundary currents in a warming climate. *Journal of Geophysical Research: Oceans*, *121*, 4928–4945. https://doi.org/10.1002/2015JC011513

Ypma, S. L., van Sebille, E., Kiss, A. E., & Spence, P. (2016). The separation of the East Australian Current: A Lagrangian approach to potential vorticity and upstream control. *Journal of Geophysical Research: Oceans*, *121*, 758–774. https://doi.org/10.1002/2015JC011133